FRB 121102 Bursts at a Constant Rate per Log Time

Elisa Tabor[1] and Abraham Loeb[2]
[1] Department of Physics, Stanford University, 452 Lomita Mall, Stanford, CA 94305, USA; etabor@stanford.edu
[2] Department of Astronomy, Harvard University, 60 Garden Street, Cambridge, MA 02138, USA; aloeb@cfa.harvard.edu
Received 2020 August 6; revised 2020 September 20; accepted 2020 September 21; published 2020 October 8

Abstract

Despite many searches for periodicity in the repeating fast radio burst FRB 121102, the underlying pattern of bursts does not appear to be a periodic one. We report a logarithmic repetition pattern in FRB 121102 in the sense that the rate falls off inversely with time for each set of bursts. This result implies that repeating fast radio burst sources are not necessarily associated with a pulsar, but rather could be caused by a different type of phenomenon that involves an equal amount of energy output per log time.

Unified Astronomy Thesaurus concepts: Radio transient sources (2008)

1. Introduction

Fast radio bursts (FRBs) are bright transients that last roughly 1 ms (Lorimer et al. 2007; Thornton et al. 2013). Based on their large dispersion measures and the observed redshifts of several of their host galaxies, most of the detected FRBs are believed to originate at extragalactic distances (Keane et al. 2016; Chatterjee et al. 2017; Tendulkar et al. 2017). Recently, the Canadian Hydrogen Intensity Mapping Experiment (CHIME), the Five-hundred-meter Aperture Spherical radio Telescope, and other surveys have been reporting many new bursts (Li et al. 2019; Fonseca et al. 2020).

Some FRBs have been found to repeat, while others have only been detected once, and we do not have enough information to know whether the two types are different populations or whether all FRBs will eventually repeat (Caleb et al. 2019; James et al. 2019). In this Letter, we will focus on the known repeaters in an attempt to understand some of the underlying properties of the engine that powers the bursts.

Two FRBs have been found to be modulated on particularly long periods. CHIME detected a 16 day periodicity in FRB 180916, with bursts arriving in a 4 day phase window, i.e., several bursts were detected over the course of 4 days and none were reported the other 12 days for several periods of this FRB (CHIME/FRB Collaboration et al. 2020; Marthi et al. 2020). The other repeater, FRB 121102, is the focus of this Letter. It is the most studied repeating FRB and was found to have a period of 157 days, with an 88 day active phase (Rajwade et al. 2020). The period was found such that every reported observation of a burst from FRB 121102 fits within an active period and every nondetection fits within an inactive period. However, there was not enough data collected to conclusively demonstrate that there could not be a smaller modulation period than that reported (see Figure 2 of Rajwade et al. 2020). Bursts from FRB 121102 originate in a star-forming region on the outskirts of a dwarf galaxy at redshift $z = 0.193$ (Bassa et al. 2017; Chatterjee et al. 2017; Marcote et al. 2017; Tendulkar et al. 2017).

Many models have been proposed to explain the sources producing the FRBs, and the most popular one for repeating FRBs describes them as pulses from magnetars, which are neutron stars with extremely strong magnetic fields (Katz 2020; Levin et al. 2020; Muñoz et al. 2020). This is motivated in part by the recently discovered FRB originating in a Galactic source

(Bochenek et al. 2020; Scholz & CHIME/FRB Collaboration 2020), which demonstrates some periodicity as well (Grossan 2020). However, the luminosity of this FRB was $\sim 10^3$ times too small for it to be of the same population as the ones detected at cosmological distances (Beniamini et al. 2020; Margalit et al. 2020). Other theoretical models that could explain periodicities involve orbital motion in binary systems (CHIME/FRB Collaboration et al. 2020; Rajwade et al. 2020) or the precession of neutron stars (Levin et al. 2020).

The organization of this Letter is as follows. In Section 2 we present the data set we used and our methods for data analysis. We describe the resulting fits to each data set in Section 3, and finally the implications of these findings in Section 4.

2. Methods

Although there exist many sets of data on bursts from FRB 121102 (Scholz et al. 2016, 2017; Spitler et al. 2016; Gajjar et al. 2018; Michilli et al. 2018; Gourdji et al. 2019; Caleb et al. 2020; Cruces et al. 2020; Oostrum et al. 2020), most sets have between 10 and 25 detected bursts in any single observation period, too few for any firm statistical inference. However, the Breakthrough Listen group was able to detect 72 additional bursts to the original 21 reported by Gajjar et al. (2018) using machine learning methods, totaling 93 points in a 5 hr period (Zhang et al. 2018). This is the data set we will be focusing on.

Any observation period must have started at a specific time, which was unlikely to be the start of the set of bursts, so we include a timescale t_0, which roughly characterizes the appearance time of the first unseen burst in the series of bursts under consideration, among our floating parameters. In analyzing the data, we used the scipy optimization CURVE_-FIT package in python[3] to develop a prediction for where the FRBs should land given each value of t_0. To find the standard deviation of these predictions, we binned the data points, evening out the Poisson fluctuations within each bin, and compared the bins against the resulting fit. We applied this algorithm to find the best-fit curve and its error for each data set.

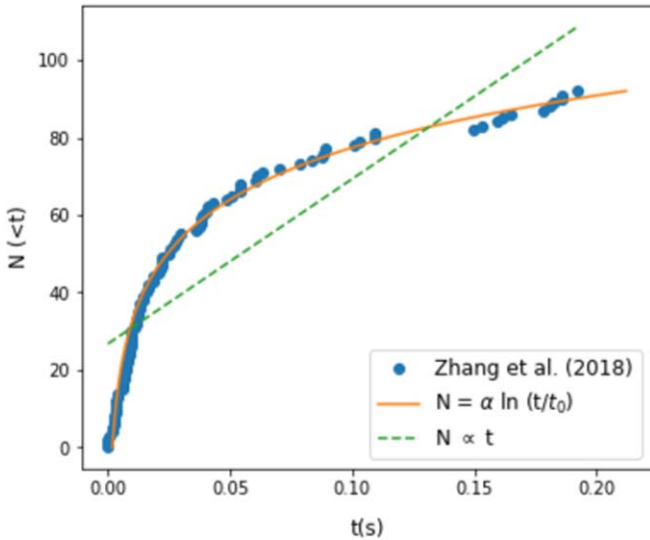[3] https://docs.scipy.org/doc/scipy/reference/generated/scipy.optimize.curve_fit.html

Figure 1. Cumulative number of bursts as a function of observed time in seconds. The orange solid curve represents the logarithmic fit to the data points from Zhang et al. (2018) based on Equation (1), with best-fit values of $\alpha = 18.1$ and $t_0 = 121$ s. The green dashed line shows an example of a periodic signal, which is unable to fit the data. The difference in their goodness of fit is illustrated by their reduced χ^2 values, as we have $\chi^2_\nu = 7.37$ for the orange solid curve and $\chi^2_\nu = 1040$ for the green dashed line.

3. Results

The best fit for the Breakthrough Listen data (Zhang et al. 2018) is presented in Figure 1. We fit the data to the formula

$$N(<t) = \alpha \ln(t/t_0), \tag{1}$$

for $t \gtrsim t_0$, with N being the number of bursts and t the time since the start of the observation period. Our best-fit values are $\alpha = 18.1^{+0.630}_{-0.663}$ and $t_0 = 121^{+20.6}_{-20.3}$ s. The first in this series of 93 bursts started when $N = 1$ at $t = e^{1/\alpha}t_0 = 128^{+21.5}_{-21.2}$ s. Since the duration of a single burst is ~ 1 ms, this implies an initial duty cycle of $\sim 10^{-5}$.

The orange solid curve in Figure 1 represents the logarithmic fit to the data points from Zhang et al. (2018) based on Equation (1), while the green dashed curve represents a periodic underlying signal. The difference in their goodness of fit is illustrated by their reduced χ^2 values, as we have $\chi^2_\nu = 7.37$ for the logarithmic fit and $\chi^2_\nu = 1040$ for the periodic fit.

Since

$$N(<t) = \alpha \ln(t/t_0) = \alpha \ln(t) - \alpha \ln(t_0), \tag{2}$$

taking the derivative with respect to $\ln(t)$ yields

$$\alpha = \frac{dN}{d\ln(t)} = t\frac{dN}{dt}, \tag{3}$$

so our final result for the burst rate of FRBs is

$$\frac{dN}{dt} = \frac{\alpha}{t}. \tag{4}$$

Figure 2 shows the confidence contours in the (α, t_0) plane, where the colors represent the standard deviation. The plot demonstrates how closely correlated α and t_0 are.

We also ran a simulation to check whether we could fit the rest of the existing data (from Zhang et al. 2018; Rajwade et al. 2020; Cruces et al. 2020) to the pattern shown in our results. In
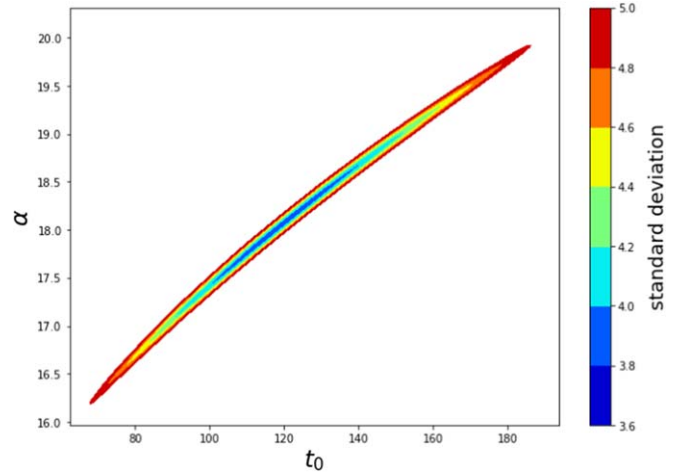

Figure 2. Contour plot demonstrating the impact of the initial timescale of the bursts (t_0) on the value of α in Equation (1), where the colors represent the standard deviation, applied to the data points from Zhang et al. (2018).

our simulations, we assumed the theoretical data would appear in sets of logarithmic curves, and that the starts of these sets would either be constant (separated by 0.2–10 days) or random (selected from a range of 0–N days where N takes on integers 1 through 5). We started from MJD 57991.41, which is the start date of the data published by Zhang et al. (2018), and we created a model set of data points that consists of curves resembling the orange solid line in Figure 1. One caveat lies in the possibility that the α and t_0 found in Figure 1 may be frequency dependent, but for the sake of this analysis we adopt a single frequency-independent value for them. Under this assumption, we were able to simultaneously compare detections at different frequencies and sensitivities by computing the error between the measured MJD and the closest predicted MJD.

In the constant separation scenario, this model set of data points was repeated every fixed period of time, which we varied as a free parameter to minimize the error relative to the time tags of the detected bursts. In the second scenario, our free parameter was the number of days the random increment could be selected from, and the starts of each set of bursts were accordingly separated by random increments from that range. When the random increment is selected from 4 or fewer days, the error is small enough that we should not rule out this model.

A histogram of the simulation for the constant separation scenario is shown in the top and middle panels of Figure 3, where the red represents real data, the black represents nondetection periods, and the gray represents the simulated set of points. The violet vertical lines demonstrate the area of the top panel that is magnified in the middle panel. For each real observed data point, we found the closest simulated point and used the difference between the two time tags as our error. Our final error per point was the norm of this set of errors (the square root of the sum of the squares divided by the number of points), and this final result is shown by the red curve in the bottom panel of Figure 3 for various separations from 5 hr to 10 days. All separations under a day gave an error better than 0.1, so we were not able to conclusively find the best possible separation between sets of bursts. We also created a random set of observations that had a uniform probability of appearing within the active periods mentioned in Rajwade et al. (2020)
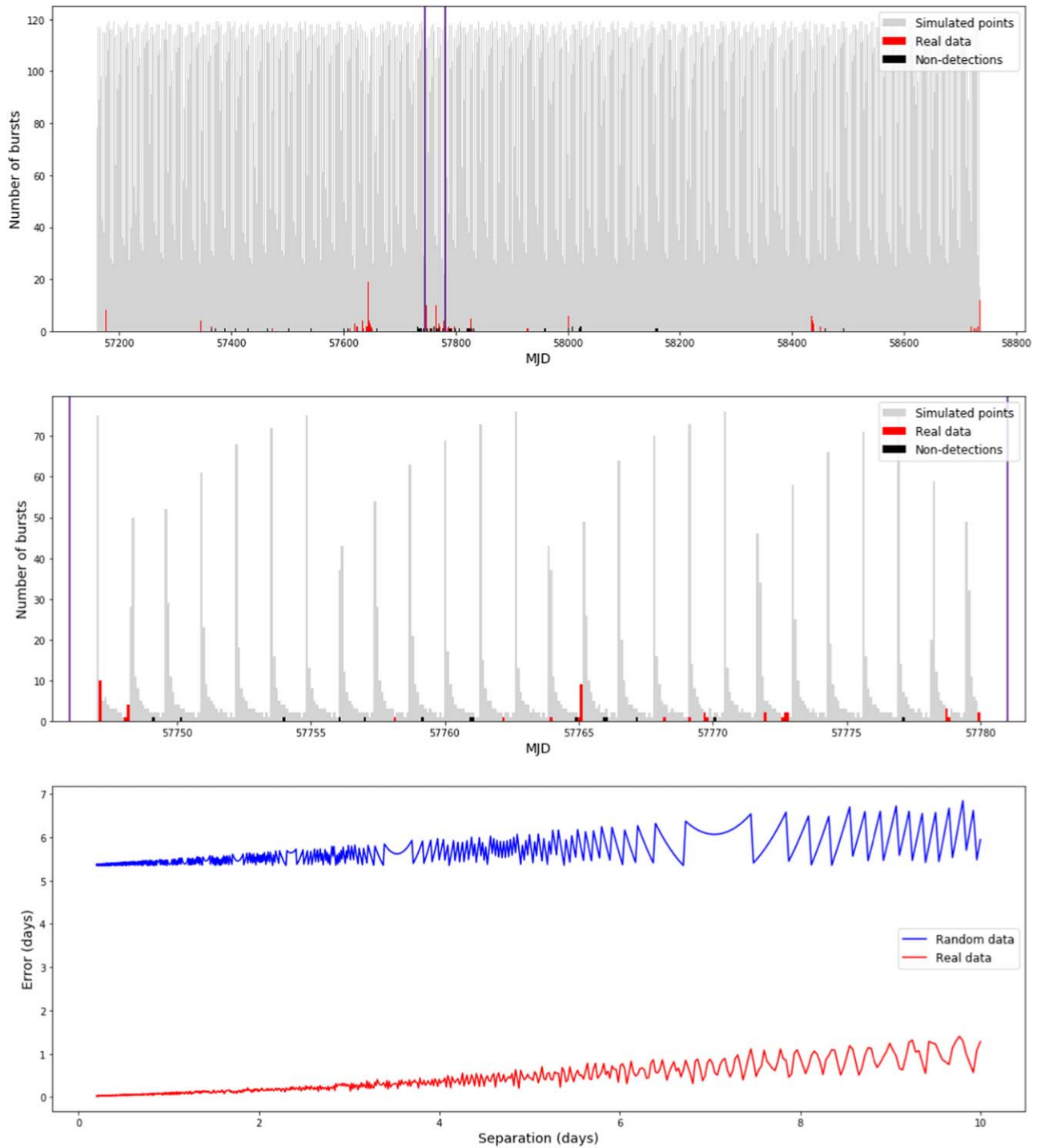
Figure 3. A simulation of a fit to the data from Zhang et al. (2018), Rajwade et al. (2020), and Cruces et al. (2020). Top and middle panels are examples of a case with a steady separation of 1.3 days between sets, where the red represents real data, the black represents nondetection periods, and the gray represents the simulated set of points. The violet vertical lines demonstrate the area of the top panel that is magnified in the middle panel. Bottom panel demonstrates the error as a function of time separation between sets of bursts for the complete activity cycle, corresponding to the top panel. The red again represents real data and the blue curve represents a random set of observations that had a uniform probability of appearing within the active periods mentioned in Rajwade et al. (2020) and Cruces et al. (2020).

and Cruces et al. (2020), which is shown by the blue curve in the bottom panel of Figure 3.

We also compared our modeled simulation against the nondetection periods published by Rajwade et al. (2020) and Cruces et al. (2020), in which no bursts were detected. Whenever the model predicts a burst in such a nondetection period, the prediction is at least off by the duration of time between the closer edge of the nondetection period and the predicted burst, so we included this as additional error in our model. We have found that there is no information in these nondetection periods in terms of error optimization.

4. Discussion and Conclusions

An implication of these findings is that FRB 121102 is not periodic, but rather it follows a logarithmic repetition pattern,

where the rate falls off as one over time for each set of bursts. This could plausibly explain the vacant, inactive regions in Figure 2 of Rajwade et al. (2020), since beyond a certain amount of time, there are so few bursts that the probability of measuring one goes to zero. However, if t_0 is on the order of hundreds of seconds, there may be many smaller sets of bursts within each period reported by Rajwade et al. (2020). Another possibility is that FRB 121102 emits equal amounts of energy per log time, but the emission pattern still follows the overall Rajwade et al. (2020) modulation periodicity of 157 days, thereby fitting the rest of the observations found over the past four to five years. More data and monitoring of the source is necessary to come to a more firm conclusion.

Another implication is that this lack of periodicity is not consistent with the idea that repeating FRBs are a type of pulsar (Beniamini et al. 2020; Muñoz et al. 2020), rather they might be caused by a different type of phenomenon that involves an equal amount of energy output per log time. This could be indicative of a process with a characteristic timescale of t_0. For example, the source of the FRB could be an object that charges up and then discharges with equal amounts of energy output per logarithmic time interval.

A potential concern with the model is that the data from Cruces et al. (2020) contains a set of 24 observations in a 7 hr period in which the rate significantly increases in the second half of the observations. Assuming the sensitivity of the data collection methods remained constant, this would imply a change in the intrinsic rate of bursting, unless within that 7 hr period one cycle of bursts ends and another begins.

A few remaining open questions are the effect of the detection threshold of the observations as there might have been many fainter bursts that were missed, possibly affecting the pattern we found, and the potential effect of frequency on the underlying burst pattern.

In conclusion, we have shown that some repeating FRBs may not send periodic bursts, rather the bursts could be arriving at a logarithmic rate. Our Equation (1) can be tested by upcoming data on repeating FRBs in the near future (Li et al. 2019; Hashimoto et al. 2020).

A roughly constant burst rate in log time was previously noted by Wadiasingh & Timokhin (2019).

ORCID iDs

Elisa Tabor https://orcid.org/0000-0002-1227-1516
Abraham Loeb https://orcid.org/0000-0003-4330-287X

References

Bassa, C. G., Tendulkar, S. P., Adams, E. A. K., et al. 2017, ApJL, 843, L8
Beniamini, P., Wadiasingh, Z., & Metzger, B. D. 2020, MNRAS, 496, 3390
Bochenek, C., Kulkarni, S., Ravi, V., et al. 2020, ATel, 13684, 1
Caleb, M., Stappers, B. W., Abbott, T. D., et al. 2020, MNRAS, 496, 4565
Caleb, M., Stappers, B. W., Rajwade, K., & Flynn, C. 2019, MNRAS, 484, 5500
Chatterjee, S., Law, C. J., Wharton, R. S., et al. 2017, Natur, 541, 58
CHIME/FRB Collaboration, Amiri, M., Andersen, B. C., et al. 2020, Natur, 582, 351
Cruces, M., Spitler, L. G., Scholz, P., et al. 2020, arXiv:2008.03461
Fonseca, E., Andersen, B. C., Bhardwaj, M., et al. 2020, ApJL, 891, L6
Gajjar, V., Siemion, A. P. V., Price, D. C., et al. 2018, ApJ, 863, 2
Gourdji, K., Michilli, D., Spitler, L. G., et al. 2019, ApJL, 877, L19
Grossan, B. 2020, arXiv:2006.16480
Hashimoto, T., Goto, T., On, A. Y. L., et al. 2020, MNRAS, 497, 4107
James, C. W., Ekers, R. D., Macquart, J. P., Bannister, K. W., & Shannon, R. M. 2019, MNRAS, 483, 1342
Katz, J. I. 2020, MNRAS, 494, L64
Keane, E. F., Johnston, S., Bhandari, S., et al. 2016, Natur, 530, 453
Levin, Y., Beloborodov, A. M., & Bransgrove, A. 2020, ApJL, 895, L30
Li, D., Zhang, X., Qian, L., et al. 2019, ATel, 13064, 1
Lorimer, D. R., Bailes, M., McLaughlin, M. A., Narkevic, D. J., & Crawford, F. 2007, Sci, 318, 777
Marcote, B., Paragi, Z., Hessels, J. W. T., et al. 2017, ApJL, 834, L8
Margalit, B., Beniamini, P., Sridhar, N., & Metzger, B. D. 2020, ApJL, 899, L27
Marthi, V. R., Gautam, T., Li, D., et al. 2020, arXiv:2007.14404
Michilli, D., Seymour, A., Hessels, J. W. T., et al. 2018, Natur, 553, 182
Muñoz, J. B., Ravi, V., & Loeb, A. 2020, ApJ, 890, 162
Oostrum, L. C., Maan, Y., van Leeuwen, J., et al. 2020, A&A, 635, A61
Rajwade, K. M., Mickaliger, M. B., Stappers, B. W., et al. 2020, MNRAS, 495, 3551
Scholz, P. & CHIME/FRB Collaboration 2020, ATel, 13681, 1
Scholz, P., Bogdanov, S., Hessels, J. W. T., et al. 2017, ApJ, 846, 80
Scholz, P., Spitler, L. G., Hessels, J. W. T., et al. 2016, ApJ, 833, 177
Spitler, L. G., Scholz, P., Hessels, J. W. T., et al. 2016, Natur, 531, 202
Tendulkar, S. P., Bassa, C. G., Cordes, J. M., et al. 2017, ApJL, 834, L7
Thornton, D., Stappers, B., Bailes, M., et al. 2013, Sci, 341, 53
Wadiasingh, Z., & Timokhin, A. 2019, ApJ, 879, 4
Zhang, Y. G., Gajjar, V., Foster, G., et al. 2018, ApJ, 866, 149